Acoustic Emission and fracture energy dissipation in notched concrete beams subjected to three-point bending tests

Acoustic Emission and fracture energy dissipation in notched concrete beams subjected to three-point bending tests

Emanuela Di Battista[1], Giuseppe Lacidogna[1], Stefano Invernizzi[1], Federico Accornero[1], Oscar Borla[1], Alberto Carpinteri[1]

[1]*Department of Structural, Geotechnical and Building Engineering, Politecnico di Torino, Italy*
E-mail: *emanuela.dibattista@polito.it, giuseppe.lacidogna@polito.it, stefano.invernizzi@polito.it, federico.accornero@polito.it, oscar.borla@polito.it, alberto.carpinteri@polito.it*

Keywords: Finite element method, Brittle fracture, Energy release, Acoustic Emission, Signals attenuation.

In this study, three-point bending (TPB) tests on notched concrete beams having different size, have been carried out to evaluate the influence of propagation distance on the AE parameters. The most representative AE parameters have been measured by sensors at different distances from the source, in order to obtain detailed information on the type of cracks as well as on the source localization. The waves frequency and the rise angle are used to discriminate the prevailing cracking mode from pure opening or sliding [1]. The cumulated number of AE events and their amplitude are used to compute the signal energy. Each signal recorded during the bending test by the first sensor has been compared with the same signal captured by the other one. For all concrete beams, an average value of the AE parameters for each sensor has been made. The AE parameters average value indicates how important the propagation distance between the two sensors is for the AE analysis. However, AE waveform parameters are effected by strong attenuation and distortion due to propagation through an inhomogeneous medium, which should not be neglected in laboratory and, in particular way, on real structures.

The AE results obtained from the three-point bending tests prove that the variation of the AE parameters during the loading process strictly depends on the specimen damage. A decrease in frequency may be provoked by large cracks progress both during tensile and sharing process, while an increase in AE signal energy content is detected approaching the final failure.

A distinct element numerical model of the beam is described and used to model the energy dissipation during the three point bending test. The model accounts for the mesostructure of plain concrete in the region closed to the central notch. Each aggregate is modeled together with the bonding of the matrix. In this way it is possible to simulate numerically the concrete crushing, as well as the tensile cracking at the aggregate interface or through the matrix and, eventually, through the inclusions [2-4]. The model is able to simulate the Acoustic Emission localization and statistics, in addition to the fracture energy dissipation, allowing for a better understanding of the ongoing phenomena.

1 INTRODUCTION

The Acoustic Emission (AE) technique is currently used during experimental tests, to investigate the fracturing behavior of materials before final failure [5,6]. In addition, this nondestructively monitoring method is useful to study the damage phenomena, to predict durability and remaining life-time in large structures [7,8].

According to this technique, it is possible to detect the transient elastic waves after any stress-induced crack propagation event inside a material. These waves can be captured and recorded by transducers applied on the surface of specimens or structural elements. The transducers are

piezoelectric sensors that transform the energy of the elastic wave in an electric signal. In this way, the AE monitoring technique gives detailed information about the type of cracks, it makes possible to localize the source crack location and to evaluate the amount of energy released during the loading process.

The connection between the mode of crack and the waves recorded depends on different factors like geometric conditions, relative orientation and propagation distance [9]. The AE waveform parameters, which have been correlated with the cracking mode, are mainly the rise time and peak amplitude, used to calculate the rise angle (RA) value [10-13], defined as the ratio of the rise time (expressed in ms) over the peak amplitude (expressed in V).

Another parameter used to characterize the cracking mode is the Average Frequency (AF) measured in kHz. The AF values are obtained from the AE ringdown count divided by the duration time of the signal. The AE ringdown count corresponds to the number of threshold crossings within the duration time.

The fracture mode is characterized by the shape of the AE waveforms. Low rise time values and high frequency are typical of tensile crack propagations which includes opposing movement of the crack sides (Mode I); whereas shear events usually result in longer waveforms, with longer rise times and lower frequency (Mode II), as shown in Fig. 1 [9]. These conditions are synthesized by the RA value [14-17].

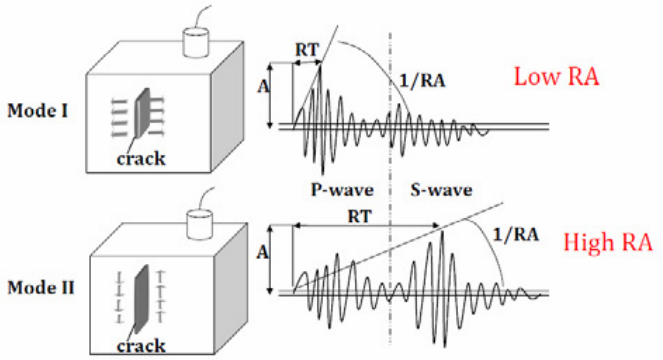

Figure 1: Typical waveforms of tensile and shear events. *A* is the amplitude and RT the rise time (time between the onset and the point of maximum amplitude) of the waveforms [9].

In the present paper, these AE parameters are acquired on notched concrete beams with different size tested in three-point bending; while their AE activity was monitored by two sensors for each beam. The sensors were placed at different distances from the notch to evaluate how the transient wave from the same fracturing event changes with the distance and to study the effect of attenuation due to different measurement points. Average values of the AE parameters recorded by each sensor during the tests were made. Afterwards, they were compared to estimate the influence of the signals propagation length for the AE analysis. An evaluation of the released AE signals energy and total dissipated energy during the tests is also calculated.

Finally, it is possible to evaluate a good correlation between the amount of cracking simulated numerically and the experimental acoustic emission counting through a finite element model.

2 EXPERIMENTAL DETAILS

Three different types of beams had been tested. A scheme of a specimen is shown in Fig. 2, where “h” is the height, “l” is the length and “d” is the deep. Their main geometrical characteristics are reported in Table 1.

A central notch of half height of the beam was made starting from the middle point at the lower side. The specimen was tested until the final failure is reached.

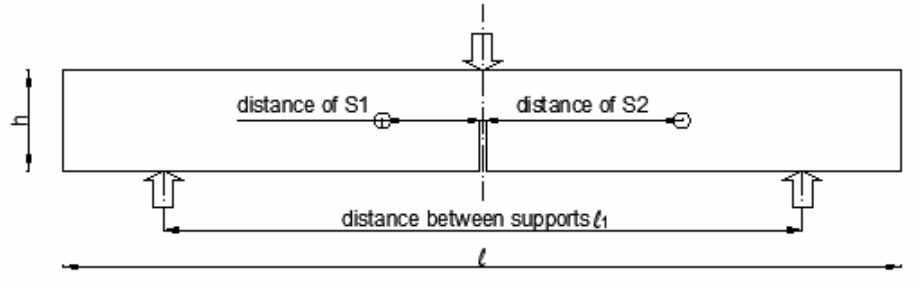

Figure 2**:** Schematic representation of the specimen tested in three point bending.

	SPECIMEN 1	SPECIMEN 2	SPECIMEN 3
Beam height h [mm]	840	1190	1450
Beam lenght l [mm]	100	200	300
Beam deep d [mm]	100	100	150
Distance between supports ℓ_1[mm]	640	990	1250
Distance of S1from the notch [mm]	37.5	150	200
Distance of S2 from the notch [mm]	112.5	300	400

Table 1**:** Main geometrical characteristics of beams.

The maximum aggregate size changed from 15 mm for the first beam to 45 mm for the third one. The water to cement ratio by mass (w/c) varied from 0.53 to 0.63; while the compressive strength had an average value of 25 MPa.

The specimens were subjected to three-point bending according to RILEM Technical Committee TC-50 on Fracture Mechanics of Concrete: "Determination of the fracture energy of mortar and concrete by means of three-point bend tests on notched beams", Draft Recommendation, Materials And Structures, Vol. 18, 1985.

The experimental test was conducted using a servo-controlled machine (MTS) with a closed loop control (Fig. 3). The monitored notched beam was conducted up to failure controlling the crack mouth opening displacement (CMOD) with an opening velocity equal to 0.002 mm/s.

During the tests, each specimen was monitored by the acoustic emission technique. AE signals are detected by two AE piezoelectric (PZT) transducer attached on the surface of the concrete specimen, sensitive in the frequency range from 80 to 400 kHz for high-frequency AEs detection. The sensors are produced by LEANE NET s.r.l. (Italy). These AE sensors, are designed to optimize weight, size, and applicability to different structural supports [8]. The connection

between the sensors and the acquisition device is realized by coaxial cables in order to reduce the effects of electromagnetic noise.

The sampling frequency of recording waveforms was set to 1 Msample/s. The data were collected by a National Instruments digitizer with a maximum of 8 channels. The AE signals, captured by the sensors, were pre-amplified of 60 dB before they have been processed, setting the acquisition threshold level up to 5 mV .

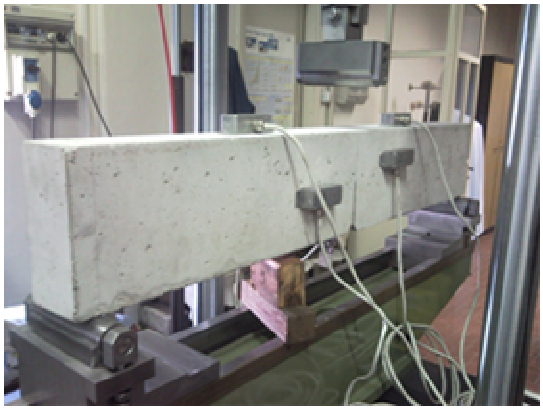

Figure 3**:** Experimental set up of the three point bending test.

3 EXPERIMENTAL RESULTS

In this section, the results of three-point bending tests carried out on concrete beams having different size are presented.

The AE technique used for the tests was based on the total number of hits detected by each sensor, but the AE analysis was limited only to the AE events. A hit is one AE transient signal received by each receiver; while one event is a group of AE hits received from a single source by two channels, of which spatial coordinates are known [10]. In this way, it is possible to compare each signal captured by the first receiver with the same recorded by the second one, even if the distance from the source changes.

For each beam, average values of the AE parameters recorded by the first sensor until the final failure have been compared to those of the second sensor.

The load vs. time diagram compared with the average values of AF and RA (for the two sensors) and cumulated AE events of the beam having dimensions 840 x 100 x 100 mm (specimen 1) is reported in Figure 3. From the mechanical point of view, the overall behavior is characterized by a normal softening post peak phase. During the test an increase in the AE events was obtained approaching the peak load.

An important AE parameter used to characterize the cracking mode is the average frequency. It decreases for the duration of the trial (Fig. 4) and also between the two receivers from 145 kHz to 102 kHz (Fig. 5a). Thus, a shift in frequencies from higher to lower values is observed.

As regards the signal amplitude, a decrease of its average value between the two sensors is expected, due to damping and scattering effects. The results obtained are reported in Fig. 5b. The average amplitude recorded by the nearest receiver is 71.3 dB; while there is a drop of about 1 dB for the second sensor.

The fracture mode criteria has been studied by means of the relationship between RA and AF values estimated for each sensor, as shown in Fig. 6a. Considering that a shift in frequencies from

higher to lower values are observed for each sensor and taking into account that the average RA values are approximately constant, but rather low (less than 1 ms/V), a dominant presence of tensile cracks seems to lead the damage evolution up to the final collapse. A matter of fact, for high frequency waves it is possible to propagate only through small inhomogeneities, whereas low frequency waves can propagate also through large inhomogeneities [7,18].

From the analysis of the energy content obtained from AE signals (Fig. 6b), it is verified that the damage evolution carries more powerful signals after the peak load. During this test, the amount of released energy, calculated by the AE signals energy, is estimated as 329.08 ms V 10^2. The value for the total dissipated energy is 0,15 J, that is computed as the area beneath the load vs. crack mouth opening displacement curve [19].

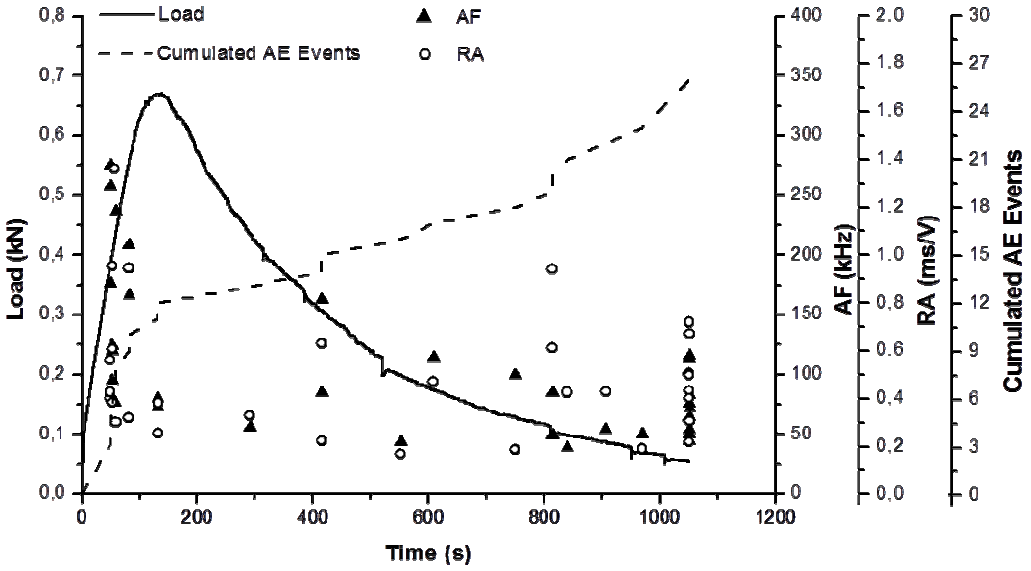

Figure 4: Specimen 1. Load vs. time diagram compared with the average values of AF, RA and cumulated AE events.

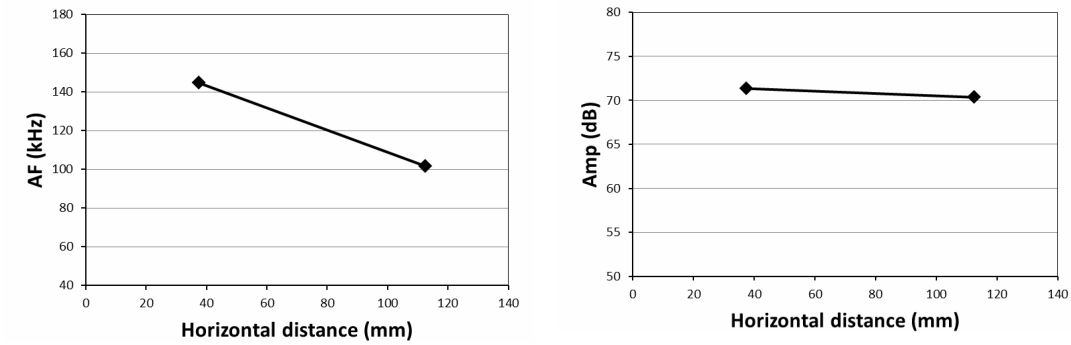

(a) **(b)**

Figure 5: Specimen 1. (a) Average AF values obtained by the two sensors. (b) Average amplitude values obtained by the two sensors.

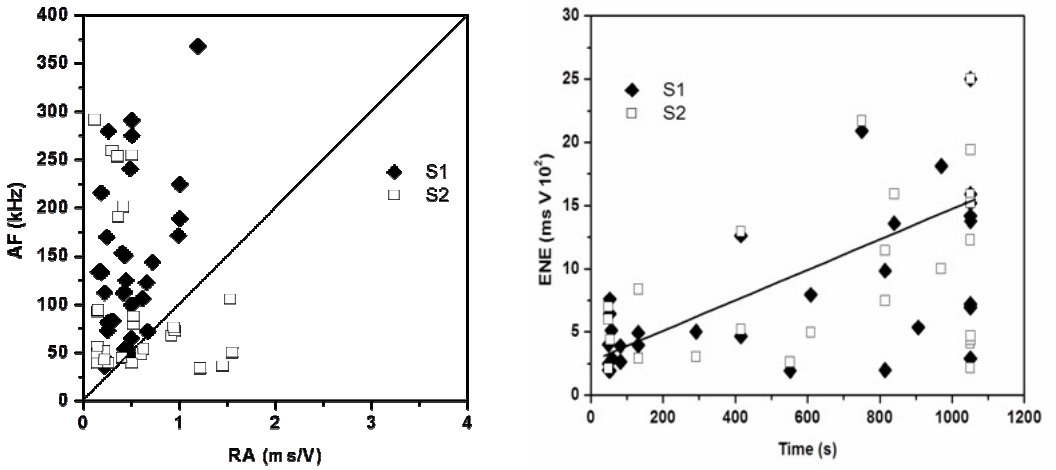

Figure 6: Specimen 1. (a) Fracture mode criteria by the relationship between RA and AF values for each sensor. (b) AE signals energy vs. time diagram.

As regards the beam having dimensions 1190 x 200 x 100 mm (specimen 2), the load vs. time diagram compared with the average values of AF and RA (for the two sensors) and cumulated AE events, is shown in Fig. 7. The overall mechanical behavior has a similar trend compared to the previous case, even if there is an increase in the cumulative number of AE events at the end of the test.

The average values of AE frequencies decreases during the loading test (Fig. 6) and also between the two sensors (Fig. 8a and Fig. 8b). from 66 kHz to 51 kHz, as well as the average amplitude. Their values change from 58.7 dB for the first sensor to 55.2 dB for the second one, due to scattering and dumping phenomena. Therefore, also in this case, a shift in frequencies and amplitude from higher to lower values had been observed. Considering the relationship between RA and AF values obtained from both sensors, it has been possible to study the type of crack. The RA values are approximately constant (Fig. 9a) but less than 1 ms/V, thus the evolution of the damage from the initial notch was dominated by a Mode I crack.

The signal energy of the AE events detected during the loading are reported in Fig. 9b, separately for each sensor. It is evident that with respect to the previous trial, the released AE signals energy is almost constant for the whole duration of the test.

The amount of the total released AE signals energy is estimated as 915 ms V 10^2; while the value for the total dissipated energy is 0.67 J.

A compression example is used to verify that the fracture mode criteria by means of the relationship between RA and AF is appropriate. The results of the test are reported in the following.

The compression test was carried out by means of a MTS servo-hydraulic press, with a maximum capacity of 1000 kN, working by a digital type electronic control unit (Fig. 13). The force applied was determined by measuring the pressure in the loading cylinder by means of a transducer. The uncertainty in the determination of the force is 1 %, which makes it a class 1 mechanical press. The specimen was arranged with the two smaller surfaces in contact with the press platens, without coupling materials in between, according to the testing modalities known as “test by means of rigid platens with friction”. The platen was controlled by means of a wire-type

potentiometric displacement transducer. The test was performed under displacement control, with the planned displacement velocity fixed at 0.001 mm/s.

Moreover, the loading process was also controlled by the circumferential strain, measured by means of a linked chain placed around the cylinder at mid-height. Such a control has permitted to completely detect the load-displacement curve, even in case of severe unstable phenomena such as snap-back. More in details, the tests were controlled by the circumferential strain up to the maximum displacement for the extensometer [1].

In Fig. 14 the load vs time diagram together with cumulated AE events, RA and AF values is reported. During the test, a shift from higher to lower frequencies involves both tensile cracks (low RA) and shear cracks (high RA), as shown in Fig. 15.

Therefore, the final collapse of the specimen is reached for different types of fracture, showing in this way, the difference with the TPB tests.

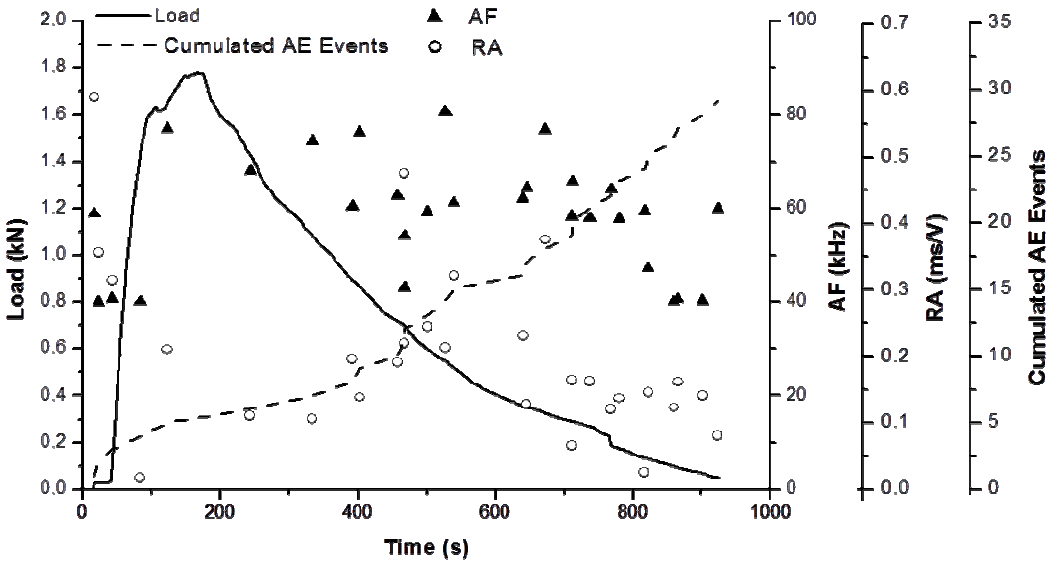

Figure 7: Specimen 2 . Load vs. time diagram compared with the average values of AF, RA and cumulated AE events.

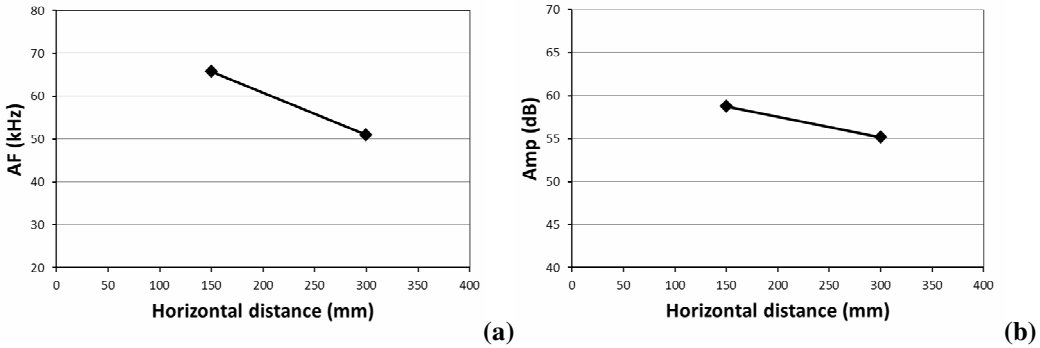

Figure 8: Specimen 2. (a) Average AF values obtained by the two sensors. (b) Average amplitude values obtained by the two sensors.

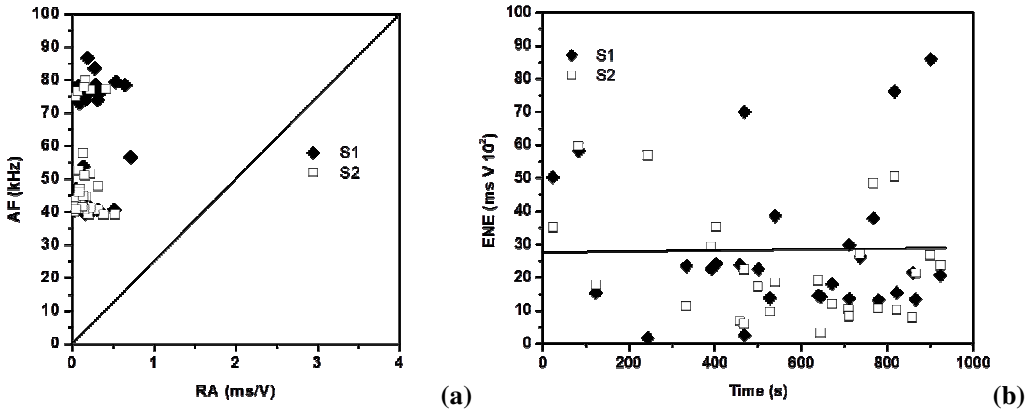

Figure 9: Specimen 2. (a) Fracture mode criteria by the relationship between RA and AF values for each sensor. (b) AE signals energy vs. time diagram.

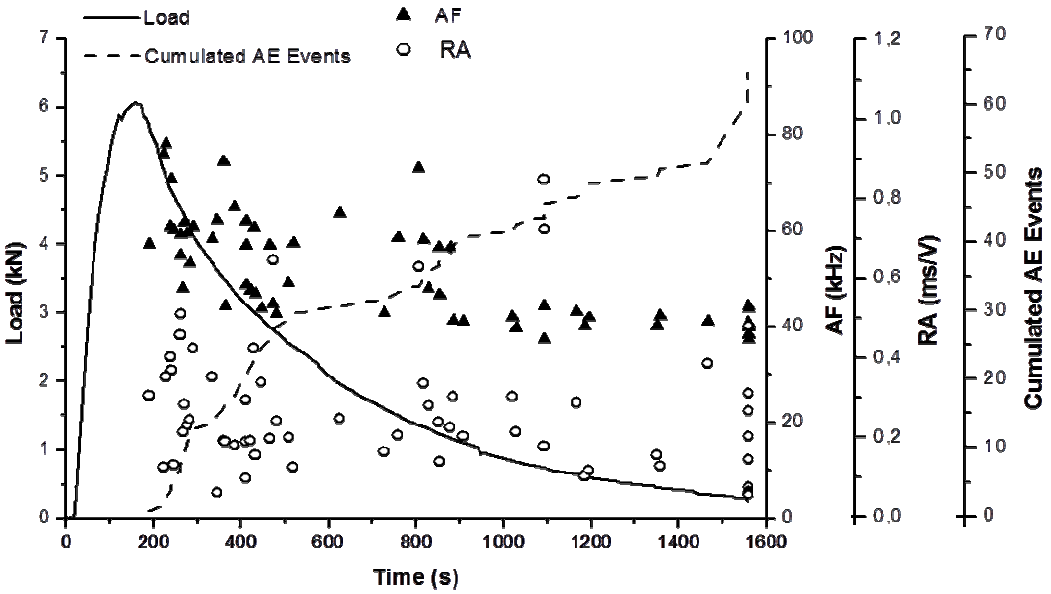

Figure 10: Specimen 3. Load vs. time diagram compared with the average values of AF, RA and cumulated AE events.

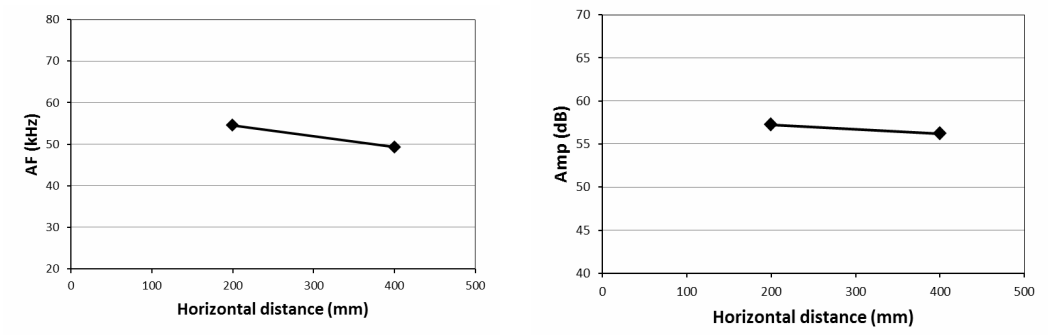

Figure 11: Specimen 3. (a) Average AF values obtained by the two sensors. (b) Average amplitude values obtained by the two sensors.

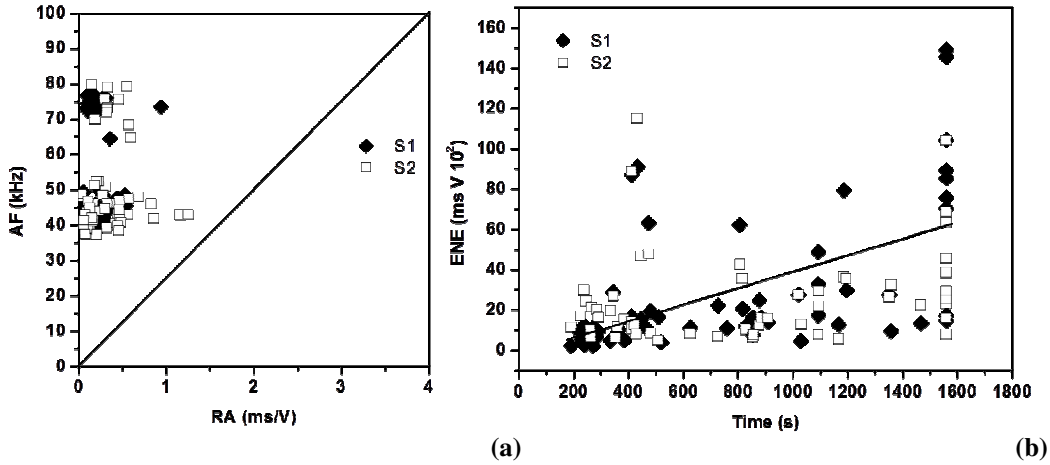

Figure 12: Specimen 3. (a) Fracture mode criteria by the relationship between RA and AF values for each sensor. (b) AE signals energy vs. time diagram.

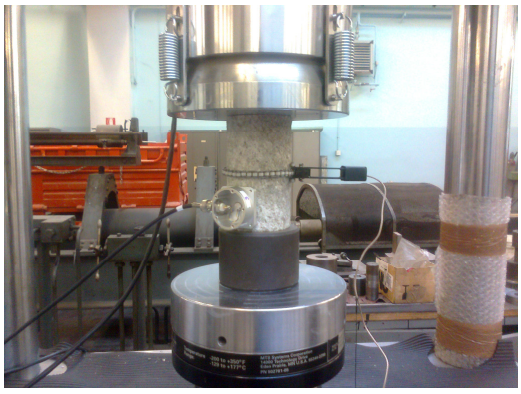

Figure 13: Experimental set up of the compression test on the concrete specimen.

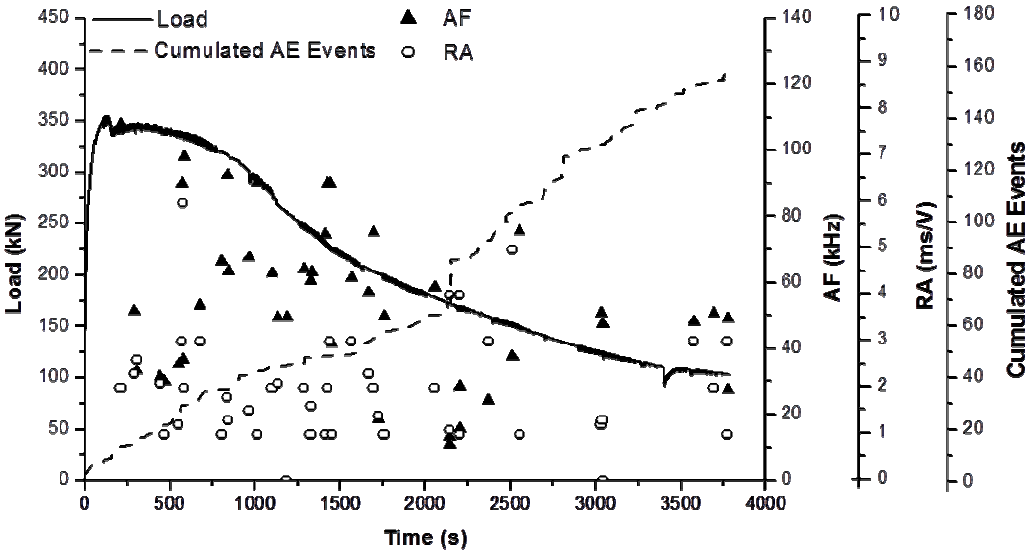

Figure 14: Load vs. time diagram compared with AF, RA values and cumulated AE events for a concrete specimen under compression.

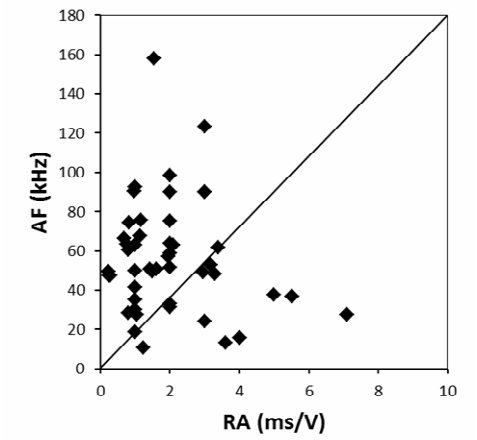

Figure 15: Fracture mode criteria with the relationship between RA and AF for a concrete specimen under compression.

Finally, it is possible compare in logarithmic scale, the energy content obtained from the AE signals with the total dissipated energy during the test for each beam, as shown in Fig. 16.

As larger is the specimen size, higher is the total dissipated energy (the area beneath the load vs. crack mouth opening displacement curve). In the same way, the number of cumulated AE events (thus the released AE signals energy) increases too. Therefore, the experimental evidence has shown that the relation between the two types of energetic parameters is not linear, but it follows a power law with an exponent equal to 1.65.

In the Fig. 17, average peak amplitude values vs. horizontal distance from the notch for all beams, is shown. A shift in amplitudes from higher to lower values is observed due to attenuation properties of the concrete material. From an experimental point of view, there is a decrease proportional to the signals propagation length (angular coefficient equal to 0.045).

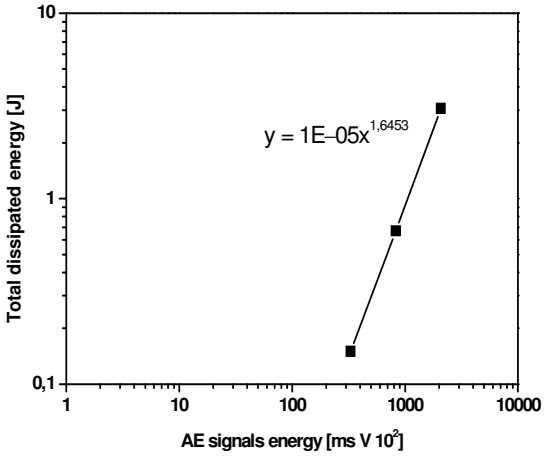

Figure 16: AE signals energy vs. total dissipated energy in logarithmic scale.

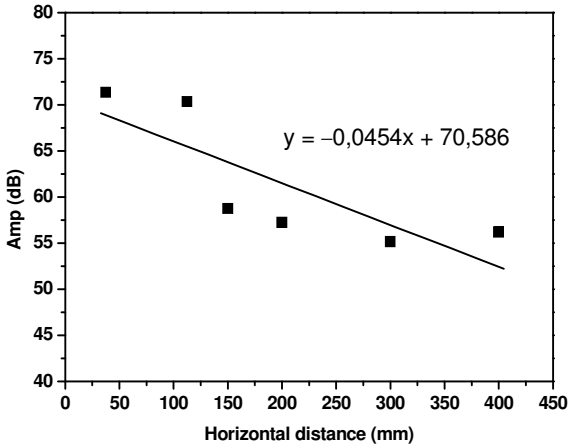

Figure 17: Average amplitude values vs. horizontal distance for all beams.

4 PARTICLE SIMULATIONS

In the previous sections of the paper it is described that during microcrack propagation, acoustic emission events can be clearly detected experimentally. Therefore, a good correlation can be found between the amount of cracking simulated numerically through finite element model and the experimental acoustic emission counting.

In particular, the simulations have been carried out with ESyS-Particle, an open source implementation of the Distinct Element Method [20]. ESyS-Particle has been developed in-house

within the Earth Systems Science Computational Centre (ESSCC) at the University of Queensland [21] since 1994.

This numerical method is based on direct integration of the Newton's motion equations with the Verlet algorithm. The normal interaction between colliding particles is linear and proportional to the particle small overlapping, whereas Coulomb friction, with both static and dynamic friction coefficients, rules the tangential interaction. In addition, bonded links are established between adjacent particles, according to the scheme in Fig. 18. The rupture of the bond is based on a fracture criterion that accounts for the axial, shear, torsion and bending behavior. The particles are filled together with the random packing algorithm LSMGenGeo [21], on the base of the maximum and minimum particle radius, which in our case correspond respectively to the maximum and minimum concrete aggregate radius (i.e. r_{max}=22.5 mm, r_{min}=7.5 mm).

An exclusion method provides that once the bonded link is broken, the frictional interaction takes place between the adjacent particles. When the maximum and minimum radius of particles are quite different, experience shows that a power-law size distribution is obtained, providing a good approximation of the actual concrete aggregate size distribution. The bending moment is applied to the simulated specimen by means of moving planes, provided that the particles closer to the platens were bonded to the moving planes.

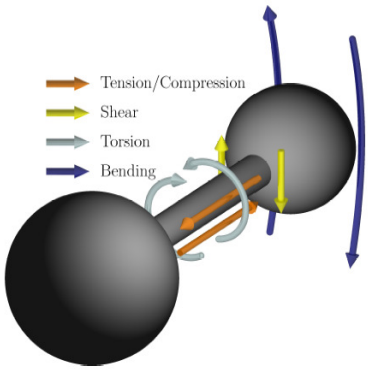

Figure 18. Scheme of the bonded interaction between two particles.

The simulations were carried out at a fixed maximum strain velocity equal to 0.001 mm/s. A viscous type damping, proportional to the particle velocity is introduced in the simulation. The choice of the damping coefficient (in our case equal to 0.02) is based on the minimum value which does not affect the stress-strain behavior. The position and velocity of each particle can be recorded at a certain integration time.

In order to limit the model complexity and the computational needs, a two-dimensional simulation of three-point bending test and AE acquisition has been performed. The particle discretization was limited to the central region of the beam, where the almost uniform bending was simulated imposing the rotation of the extreme sections (shown in red in Fig. 19a). The initial notch is obtained removing the corresponding bonds. As soon as the bonds between particles reach the failure limit, they are removed, and the crack proceeds to the extrados of the beam (Fig. 19b).

In the present study, special attention was paid to the simulation of the temporal scaling of the acoustic emission, rather than to provide a detailed interpretation of the experimental test. Nevertheless, the mechanical parameters adopted in the analysis were chosen to better interpolate the experimental strength in the whole dimensional range.

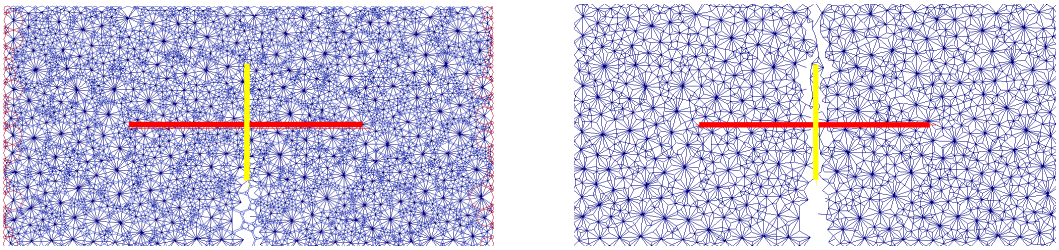

(a) (b)

Figure 19: Three point bending test: initial configuration (a); final configuration (b).

The finite element model was developed to confirm the experimental results. It can be used for TPB, compression and tensile loading tests [2-4].

Further analyses are necessary to investigate the effect of the simulation dimensionality, and to obtain a better parameter calibration of the model.

5 CONCLUSIONS

The present study discusses about the influence of propagation length on AE parameters in TPB tests on notched concrete beams having different sizes.

The main AE parameters have been measured by two sensors positioned at different distances from the notch. Afterwards each signal recorded during the loading by the first receiver has been compared with the same signal captured by the other one.

For all beams a shift from higher to lower frequencies has been observed. Considering also that the RA values are commonly low, there is a dominance of tensile crack propagations which includes opposing movement of the crack sides (Mode I). Since the longitudinal waves are the fastest type, the delay in each AE signal between longitudinal and shear waves grows with the increasing of the distance.

As regards the peak amplitude, a little decrease between the two sensors and on the propagation distance on the AE parameters has been monitored. This is due to attenuation and distortion through an inhomogeneous medium. Obviously these phenomena are attenuated on laboratory specimens; while they have a greater effect on real structures because the propagation lengths of acoustic waves are longer. The sensors have to cover a bigger area, so the AE parameters are subjected to a more evident dissipation mechanism. It can be studied in the future to obtain correct results as regards the mode of cracking also for big structures.

Moreover, it is possible to say that the amount of AE signals and total dissipated energy is bigger for larger specimens. These energies are related together according to a power law and considering the amplitude attenuation phenomenon, this law can be improved with more tests.

Finally, a finite element method is used to simulate numerically the concrete crushing, as well as the tensile cracking at the aggregate interface or through the matrix and through the inclusions in TPB tests. The model, able to simulate the Acoustic Emission localization and statistics, in addition to the fracture energy dissipation, also allows a better understanding of the experimental tests.

Aknowledgements

The authors gratefully acknowledge the support of ALCIATI Ltd (Vigliano d'Asti-Italy) for supplying the research materials.

References

[1] Carpinteri, A., Corrado, M. and Lacidogna, G. "Heterogeneous materials in compression: Correlations between absorbed, released and acoustic emission energies". *Engineering Failure Analysis* **33**:236–250 (2013).

[2] Invernizzi, S., Lacidogna, G., Carpinteri, A. "Particle-based numerical modeling of AE statistics in disordered materials" *Meccanica,* , **48**(1): 211-220 (2013).

[3] Invernizzi, S., Lacidogna, G., Carpinteri, A. "Scaling of fracture and acoustic emission in concrete". *Magazine of Concrete Research,* **65**(1), 1–6, (2013).

[4] Carpinteri, A., Lacidogna, G., Invernizzi, S., Manuello, A., "Particle simulation of AE statistics and fracture in concrete TPB test ". *Proc. of 13th International Conference on Fracture,* June 16–21, 2013 / Beijing – China (2013).

[5] Ohtsu, M., "The history and development of acoustic emission in concrete engineering". *Mag. Concr. Res.* **48**:321-330 (1996).

[6] Grosse C. and Ohtsu M., "Acoustic Emission Testing", Springer (2008).

[7] Carpinteri, A., Lacidogna, G. and Pugno, N. "Structural damage diagnosis and life-time assessment by acoustic emission monitoring". *Eng. Fract. Mech.* **74**:273-89 (2007).

[8] Carpinteri, A., Lacidogna, G., Manuello A., Niccolini G. "Acoustic emission wireless transmission system for structural and infrastructural networks". *Proc. VIII International Conference on Fracture Mechanics of Concrete and Concrete Structures FraMCoS-8, J.G.M. Van Mier, G. Ruiz, C. Andrade, R.C. Yu and X.X. Zhang (Eds)*, March 10-14, 2013 / Toledo – Spain (2013).

[9] Aggelis, D.G., Mpalaskas A.C., Ntalakas D. and Matikas T.E. "Effect of wave distortion on acoustic emission characterization of cementitious materials". *Construction and Building Materials,* **35**:183-190 (2012).

[10] RILEM Technical Committee TC212- ACD. "Acoustic Emission and related NDE techniques for crack detection and damage evaluation in concrete: Measurement method for acoustic emission signals in concrete". *Mater. Struct.*, **43**:1177-81 (2010).

[11] RILEM Technical Committee TC212- ACD. "Acoustic Emission and related NDE techniques for crack detection and damage evaluation in concrete: Test method for damage qualification of reinforced concrete beams by Acoustic Emission". *Mater. Struct.* **43**:1183-6 (2010).

[12] RILEM Technical Committee TC212- ACD. "Acoustic Emission and related NDE techniques for crack detection and damage evaluation in concrete: Test method for classification of active cracks in concrete by Acoustic Emission". *Mater. Struct.* **43**:1187-9 (2010).

[13] RILEM Technical Committee TC212- ACD. "Acoustic Emission and Related Non-destructive Evaluation Techniques for Crack Detection and Damage Evaluation in Concrete". Final Report of RILEM Technical Committee 212 ACD (2010).

[14] Soulioti, D., Barkoula, N.M., Paipetis, A., Matikas, T.E., Shiotani T. and Aggelis, D.G. "Acoustic Emission behavior of steel fibre reinforced concrete under bending". *Constr. Build. Mater*. **23**:3532-6 (2009).

[15] Ohno, K. and Ohtsu, M. "Crack classification in concrete based on Acoustic Emission". *Constr. Build. Mater*. **24**:2339-46 (2010).

[16] Aggelis, D.G. "Classification of cracking mode in concrete by Acoustic Emission parameters". *Mech. Res. Communications* **38**:153-7 (2011).

[17] Aldahdooh, M.A.A. and Muhamad Bunnori, N. "Crack classification in reinforced concrete beams with varying thicknesses by mean of acoustic emission signal features". *Construction and Building Materials,* **45**:282-288 (2013).

[18] Landis, E.N. and Shah, S.P. "Frequency-dependent stress wave attenuation in cement-based materials". *J. Eng. Mech.* **121**:737-43 (1995).

[19] RILEM 50-FMC Committee, "Determination of the fracture energy of mortar and concrete be means of three point bend tests on notched beams". *Mater. Struct.* **18**:286-90 (1986).
[20] https://twiki.esscc.uq.edu.au/bin/view/ESSCC/ParticleSimulation
[21] https://launchpad.net/esys-particle/